Strain-Induced Modulations in the Surface Morphology of Heteroepitaxial Layers

A.G. Cullis

Introduction

The growth of semiconductor heteroepitaxial layers is assuming ever greater importance due to the demands of modern electronic-device fabrication. Furthermore although low-strain heterosystems such as AlGaAs/GaAs remain the basis of many device structures, there is an increasing trend also to use more highly strained combinations such as InGaAs/GaAs and SiGe/Si. However the growth of the latter epitaxial systems must be approached with great care in order to achieve the optimum layer structural quality. Of course for any given alloy-layer composition, interfacial misfit defects in general will be introduced when the layer thickness exceeds a critical value, as originally described by Frank and van der Merwe,[1] and Jesser and Matthews.[2] (See the article by F.K. LeGoues in this issue for more general considerations of misfit-defect introduction.) In addition the morphology of such strained layers must be given very careful attention. It is the purpose of this article to examine our current understanding in this latter area.

When any epitaxial layer is grown, initially it might be expected that a flat surface would result under ideal growth conditions when internal defects have been eliminated. This would be expected to minimize the surface step density and hence the surface energy. However nature has a way of confounding our simplest expectations and while for homoepitaxial layers in the absence of kinetic effects this expectation virtually can be realized, the presence of strain in a heteroepitaxial system can severely affect the observed layer morphology.

Theoretical Considerations of Morphology-Related Strain Relief

The first theoretical treatment of morphological instability driven by stress in solids was presented by Asaro and Tiller[3] and related to stress-corrosion cracking. Description of the stress-driven instability relevant to a range of other circumstances appeared subsequently[4–9] and in particular, formulation in the context of epitaxially strained solid films was provided.[10–17]

At a phenomenological level, the driving force for the formation of nonplanar surfaces is as follows. Figure 1 shows in diagrammatic form a film compressively strained upon a substrate where surface distortions are present as undulations with relatively rounded peaks and groove- or cusplike troughs. As will be seen in the following, this type of morphology can be formed in many experimental situations. The vertically aligned lattice planes are also shown, and it is immediately clear that the unconstrained lateral edges of the surface mounds allow these planes to dilate by lateral expansion. There is then partial elastic stress relief of the epitaxial material within each mound, and this can be quantitatively modeled using finite-element analysis.[18] However a consequence of this relaxation is that there is a complementary additional compression of the lattice planes at the locations of the surface grooves. Nevertheless this latter compression is very localized so that the volume of material subjected to additional stress is much less than the volume experiencing partial stress relief. Overall there can be a reduction in the free energy of the system due to the formation of these morphological distortions.

One very important additional parameter, which must be taken into account before it is possible to assess the stability of a strained layer, is the surface energy. As mentioned previously, a flat layer might be expected to represent the minimum energy condition. When a surface distortion is introduced, steps are created so that the area and energy of the surface increases. Indeed the larger the distortion, the larger the surface area and potentially, the larger the number density of steps. Therefore this factor inhibits surface roughening until the free-energy reduction in the system by stress relief outweighs the free-energy increase due to surface-area increase and step forma-

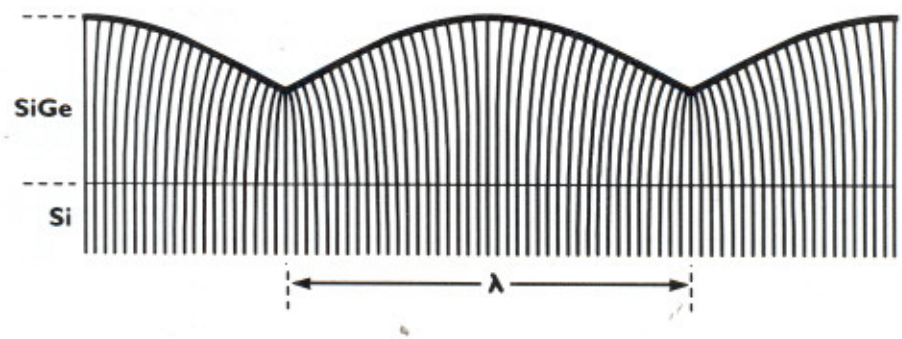

Figure 1. Diagram showing elastic distortion of vertical lattice planes in a morphologically undulating heteroepitaxial layer under compressive stress upon its substrate.

tion. Within this model, the surface undulations would actually form by migration of surface-deposited atoms under the influence of strain-induced chemical potential gradients.

Based upon the scenario just outlined and assuming on an *a priori* basis correlated sinusoidal fluctuations in total layer thickness and strain, elementary theory[14] predicts that the following inequality, relating bulk and surface energy terms, should be approximately satisfied as follows:

$$t/\lambda^2 < Y\varepsilon_0^2/4\gamma\pi^2 \qquad (1)$$

where t is the epitaxial-layer amplitude of undulation, λ is the wavelength of undulation, Y is Young's modulus for the epitaxial material, ε_0 is the basic mismatch strain, and γ is the surface free energy per unit area. Experimental results[14] taken from the SiGe/Si system and relating t/λ^2 to ε_0^2 (or to the square of the Ge fraction x) are plotted in Figure 2. The plot linearity observed strongly indicates the fundamental significance of the balance being achieved between surface and volume energy terms, as expected from the basic phenomenological arguments. However to obtain deeper insight, it is essential to determine the detailed structural characteristics of the undulating epitaxial surfaces.

Experimental Observations of Surface Morphological Undulations

Compressively strained epitaxial layers of $Si_{1-x}Ge_x$ alloy grown on Si substrates by a range of techniques, including molecular beam epitaxy (MBE) and chemical vapor deposition (CVD), exhibit broadly similar characteristics of morphology evolution. Alloy layers grown at relatively low temperatures (≤700°C) and low Ge concentrations ($x \leq 0.15$) generally show planar surface morphology. However alloy layers grown at higher temperatures and x values are strongly susceptible to surface roughening ($x = 1$ would correspond to ~4.2% misfit). This is illustrated in Figure 3, which shows[19,20] an atomic-force-microscopy (AFM) image of a typical roughened epitaxial surface, in this case of $Si_{0.81}Ge_{0.19}$ alloy. The roughening takes the form of surface ripples that lie along orthogonal ⟨100⟩ directions, as differently oriented groups arranging themselves into domains with dimensions of several microns. The precise form of the ripple structure depends upon the alloy composition (x) and other growth parameters.[21,22] For the example given in Figure 3, the ripples have a wavelength of 270 nm and peak-to-trough heights of 20–40 nm. This structure is particularly easily seen in cross-sectional transmission electron microscope (TEM) images, such as presented in Figure 4. This shows clearly the profile of the ripples. It is evident that there are many similarities to the outline previously given in Figure 1. In fact the surface ripples exhibit a strong tendency to facet[21,23] on inclined {105} planes with ~11° slopes, previously seen[24] on epitaxial Ge "hut" clusters.

It is very important to determine whether the presence of the surface ripples allows elastic strain relief to occur as in the model given in Figure 1. This is conveniently achieved by imaging the ripples in plan view using strain-sensitive contrast in the TEM. A typical region of SiGe ripples is shown in Figure 5a. When these are imaged using individual 400-type reflections, only the sets of ripples perpendicular to the g-vector of the particular operating reflec-

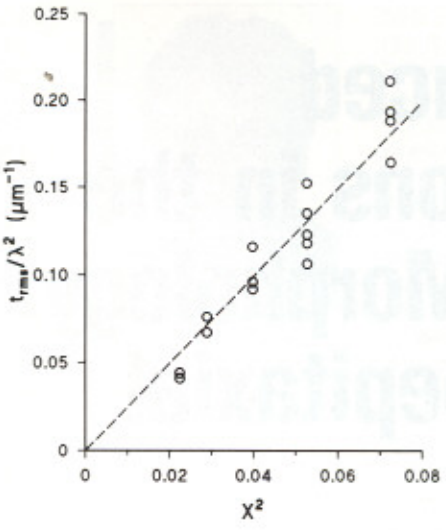

Figure 2. Atomic-force-microscopy measurements of t_{rms}/λ^2 plotted against (Ge fraction x)^2 for epitaxial SiGe layers on Si. (After Pidduck et al.[14])

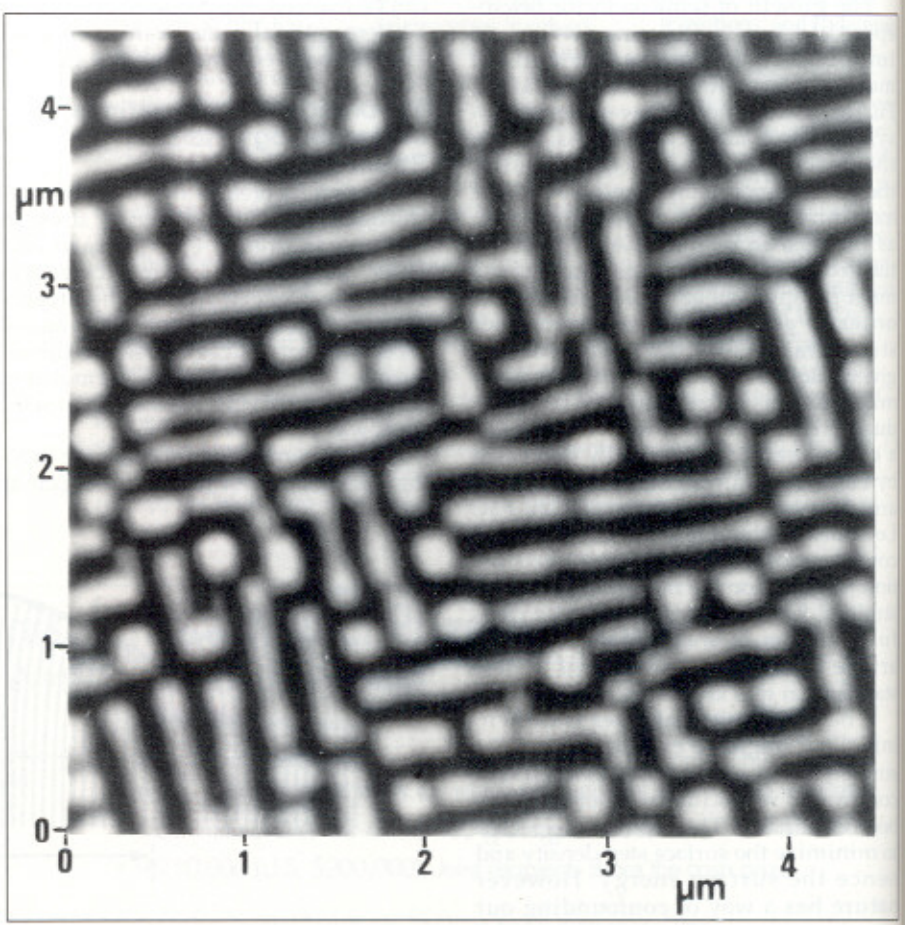

Figure 3. Atomic-force-microscopy image of an uncapped $Si_{0.81}Ge_{0.19}$ alloy layer surface showing interlocking ⟨100⟩-aligned ripple structure. (After Cullis et al.[20])

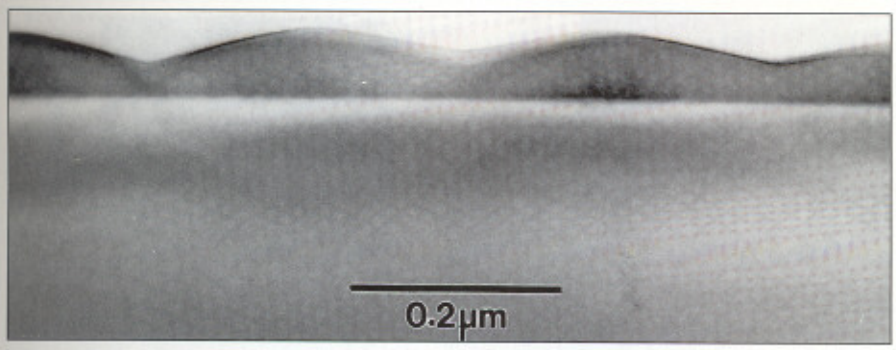

Figure 4. Cross-sectional [100] quasikinematical image of an uncapped $Si_{0.81}Ge_{0.19}$ layer showing alloy surface ripples. (After Cullis et al.[20])

tion are in contrast (Figures 5b and c). This immediately confirms that a strain gradient is directed normal to the ripple rows. Furthermore careful analysis[20] of this image contrast demonstrates that the lattice-plane bending is precisely of the form anticipated in Figure 1. Quantitative contrast measurements[23] demonstrate that the elastic relaxation is essentially complete at the surface of each ripple crest. Thus the presence of the ripples provides substantial elastic relaxation in the heteroepitaxial system.

Since the ripple sidewalls tend to facet, as already pointed out, the troughs are sharper than would otherwise be expected. Certain theoretical treatments[16,17,25] predict that the formation of the troughs can be an unstable process and that once initiated, deep cusps may form in the grown layer. A number of observations show that the depth and sharpness of the troughs can vary considerably but in one case,[25] a phenomenon approaching cusp formation has been observed. As illustrated in Figure 6, a sequence of Ge marker layers in a SiGe alloy demonstrates that a sharp depression formed in the layer at one stage of growth but subsequently filled in. It is possible that this report shows cusp formation, though it is predicted that such features should dissipate only if the local stress is reduced by dislocation nucleation. This was not observed in this case though, as will be described in the next section, well-correlated defect formation has been found under other circumstances.

Roughening phenomena directly comparable to those just described have been observed in other epitaxial systems. The most detailed studies have been carried out for the growth of compressively strained $In_xGa_{1-x}As$ alloys on GaAs. Work over a number of years has shown that for higher x alloys, initial growth takes place by the Stranski-Krastanov mechanism[26–29] in which islands of deposit are formed after a small amount of initial planar growth. For an alloy with $x = 0.25$ and deposited up to a 5-nm thickness at a temperature of 580°C, typical elongated islands are shown[30,31] in the AFM image of Figure 7a. However as the layer thickness is increased, the islands expand and join together to form, at 10-nm thickness, an array of linear ridges (Figure 7b). Further increase in the thickness to 20 nm (Figure 7c) yields a layer that exhibits an array of mounds and ridges of 10–20 nm height and up to 100 nm spacing. These have the appearance of interacting ripples and run in a chevron pattern about the [011] axis, often with near ⟨001⟩ alignment. Cross-sectional images in the TEM (Figure 8) emphasize the appearance as faceted ripples, and once again it is possible to demonstrate[31] by TEM measurements that the strain variations across these features are in accord with the model of Figure 1. Thus the formation of well-developed ripples in a number of heteroepitaxial systems has been shown to contribute strongly to stress relief in the films.

The precise manner in which stress-relieving ripples evolve appears clearest for the $In_xGa_{1-x}As$ alloys where as has been shown, coalescence of initial growth islands forms an undulating array that progressively changes in character to that of interacting ripples. The initial islands experience considerable stress relief by expansion at their edges in a manner related to that previously seen[32] for growth islands of Ge on Si substrates. The strain gradients across the island or ripple structures drive surface atom diffusion currents that generate the observed surface distortions. In principal, diffusing constituent atoms with different sizes will exhibit maximum stability in different parts of the structures due to the strain variations. This would be expected to lead to local changes in epitax-

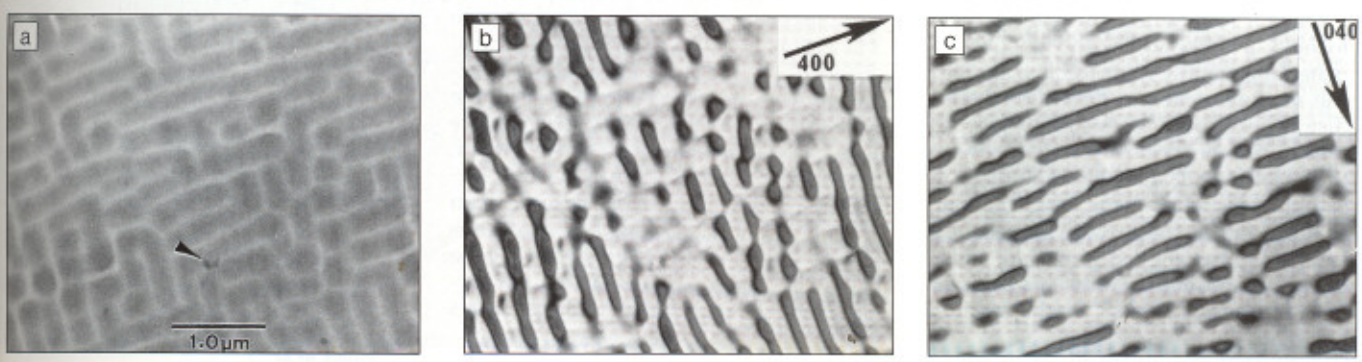

Figure 5. Plan-view transmission-electron-microscopy (TEM) images (bright-field) of the same area of a $Si_{0.81}Ge_{0.19}$/Si sample showing variation of ripple contrast with change in Bragg reflecting conditions: (a) quasikinematical, (b) strong-beam, $\mathbf{g} = 400$, and (c) strong-beam, $\mathbf{g} = 040$. (After Cullis et al.[20])

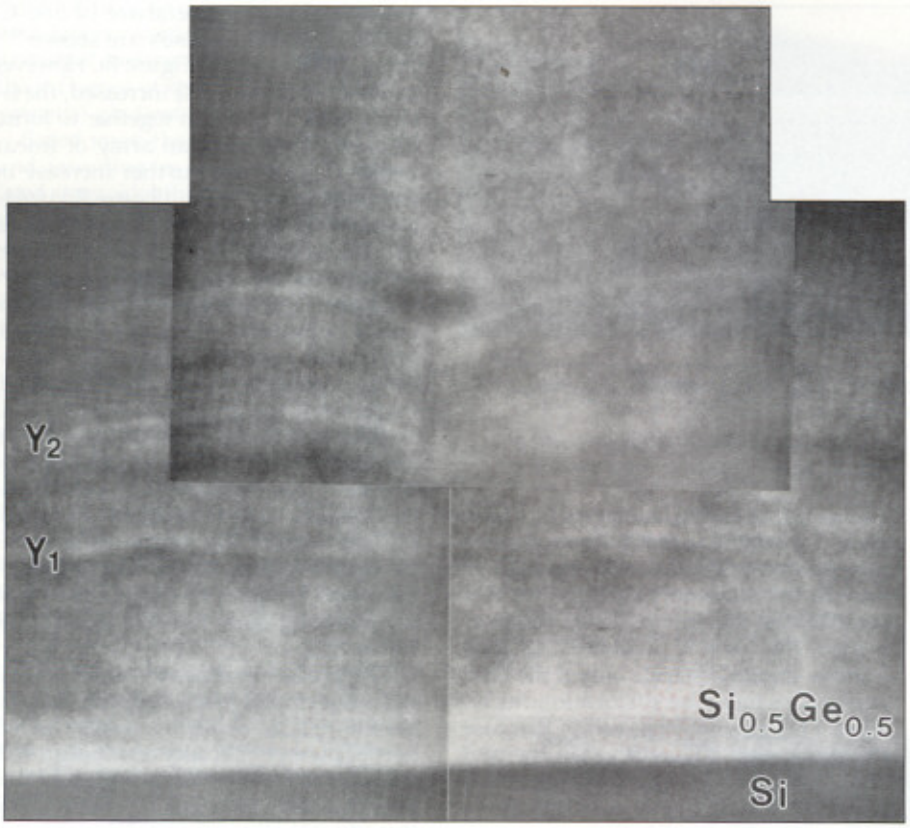

Figure 6. [110] Z-contrast image of a $Si_{0.5}Ge_{0.5}$ alloy layer grown at 400°C with 0.25-nm Ge marker layers (e.g., at Y_1 and Y_2) deposited at intervals. (After Jesson et al.[25])

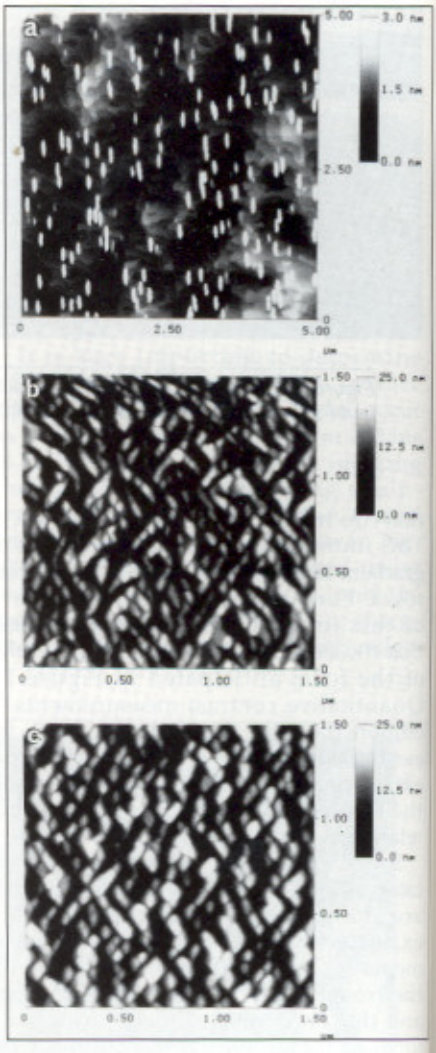

Figure 7. Atomic-force-microscopy images of $In_{0.25}Ga_{0.75}As$ layers grown at 580°C: (a) 5-nm thickness showing growth islands, (b) 10-nm thickness showing aligned linear undulations, and (c) 20-nm thickness showing a dense interacting array of islandlike ripples. (After Cullis et al.[31])

Figure 8. Cross-sectional 400 image of an $In_{0.25}Ga_{0.75}As$ layer grown on GaAs at 580°C (interface-arrowed) showing a ripplelike structure. (After Cullis et al.[31])

ial alloy concentration. These have now been directly measured[33] in rippled SiGe films on Si by use of electron nanoprobe analysis in combination with energy-dispersive x-ray microanalysis. In this way, it has been found that the concentration of Ge in ripple-peak regions where there is a lattice expansion is greater than in ripple-trough regions where there is increased compression.

Once a roughened surface has been formed, overgrowth with the substrate material generally leads to rapid smoothing of the surface undulations[20] since distortion in ripple crests no longer provides an energy gain for the growing film. However despite the smoothing, residual local lattice-plane distortions are still present at the growth surface and can lead to the aligned growth of subsequently deposited islands[34] or undulating continuous layers[35] of the strained material.

A further important point to note is that the examples of heteroepitaxial-layer roughening given thus far are in systems with compressive internal stress. While the general theory outlined earlier indicates that there should be no distinction between systems with compressive and tensile stress, more recent theoretical investigations[36] suggest that systems with tensile stress could be more resistant to roughening. Recent work[37] on a comparison of the $Si_{0.5}Ge_{0.5}$/Si and $Si_{0.5}Ge_{0.5}$/Ge systems has shown that while roughening occurs in the former (compressively strained) case, no roughening is seen in the latter system with tensile strain. Molecular-dynamics modeling has attributed[37] this observation to an increase in energy of a particular type of surface step under conditions of tensile strain, such that the magnitude of overall surface energy prevents deviations from surface planarity. It has also been observed[38] that other systems with tensile strain, such as InAlSb/InSb, exhibit surface planarity despite having high levels of built-in strain.

Misfit-Defect Formation

As was outlined previously, the formation of ripples upon a compressively

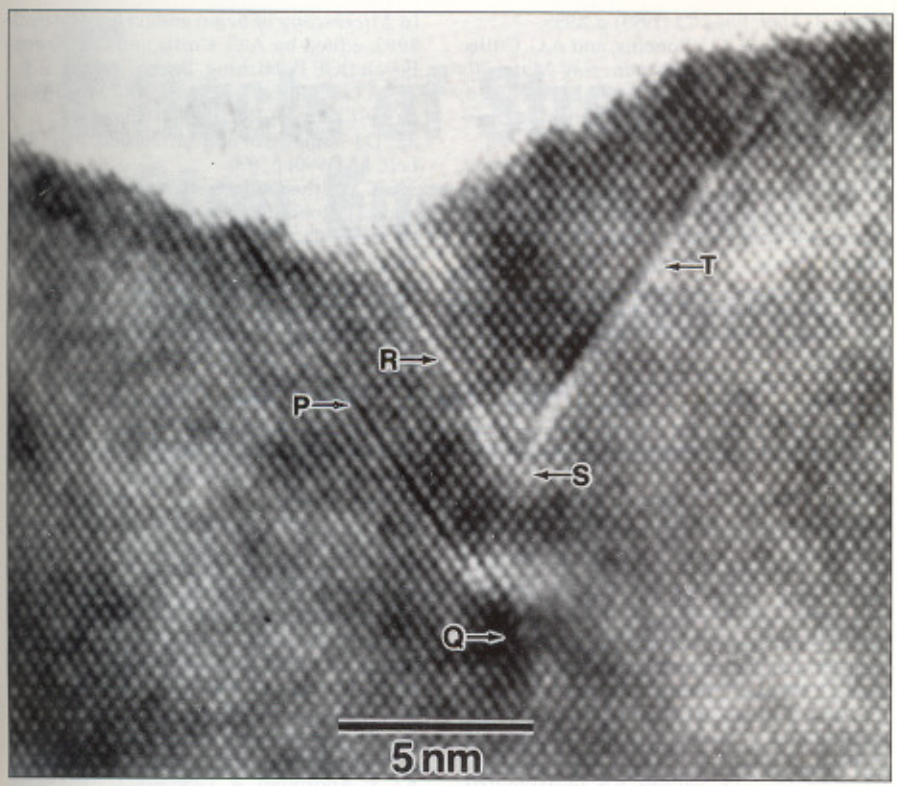

Figure 9. Cross-sectional high-resolution TEM image, [011] surface normal, showing misfit defects nucleated at a surface ripple trough in an $In_{0.25}Ga_{0.75}As$ alloy: intrinsic stacking fault (P) bounded by Frank partial dislocation (Q), and stacking fault (R) bounded by stair-rod dislocation (S) leading to secondary fault (T). (After Cullis et al.[41])

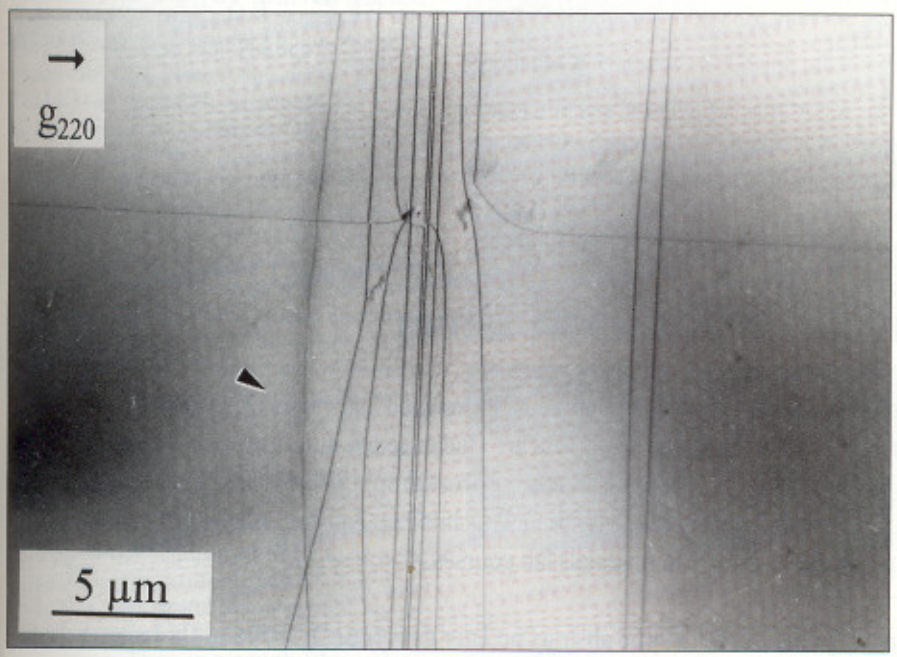

Figure 10. Plan-view TEM image of a $Si_{0.97}Ge_{0.03}$ alloy layer grown on Si by liquid-phase epitaxy, showing a bunch of 60° dislocations aligned along a ripple trough (light region). (After Albrecht et al.[44])

strained layer produces crests that are elastically stress-relieved with intervening troughs at which there is an additional local compression. Due to faceting[23] of the ripple sidewalls, the radius of curvature of the troughs may be quite small so that they resemble grooves or cusps. This sharpening of the structure leads to a further enhancement of local stress. It has been predicted[23,25,39,40] that this type of stress concentration should lead to misfit-dislocation source behavior by lowering the barrier to dislocation nucleation. Recently this process has been directly observed[31,41] at individual ripple troughs in the InGaAs/GaAs system. A direct correlation has been obtained between the location of strained ripple troughs and the nucleation of individual misfit-dislocation segments. Initial misfit defects formed are shown in the high-resolution TEM image of Figure 9. The most prevalent strain-relieving defects that occur at this very early stage of relaxation are intrinsic faulted Frank dislocation half loops,[41] formed presumably by vacancy aggregation (or interstitial emission). Other defects, such as the fault pair also shown in Figure 9 and commonly observed Lomer dislocations, can be formed from such Frank loops by basic lattice reactions.[41] This in particular provides a mechanism for the formation of sessile Lomer dislocations, which is an alternative to simple dislocation burial.[42]

It is of course also possible that misfit dislocations will be introduced into strained layers by the slip mechanism,[25,43] due to energy-barrier lowering at trough locations. Bundles of perfect 60° dislocations have been seen[44] to lie along pronounced troughs in SiGe layers grown on Si by liquid-phase epitaxy (Figure 10), suggesting that the dislocations may have been nucleated at these locations. Of course dislocations, once formed, are known to modify the local surface morphology[23,44,45] so that it would be important to make observations at a very early stage of dislocation formation. Surface ripple rearrangements caused by underlying dislocations can be quite dramatic and, for example, rows of islandlike mounds have been seen over underlying dislocations in annealed SiGe/Si samples.[45] Large stress concentrations have been identified at the grooves or cusps between such mounds. This work[45] specifies these locations as potential defect multiplication sources. Further details of these and related studies are discussed in the article in this issue by Jesson et al.

Conclusions

The observations described here emphasize the importance of morphological distortions in determining the stress relief behavior of large-misfit heteroepitaxial systems. Furthermore these studies are revealing new dislocation-source behavior directly attributable to the undulating layer morphology. Overall, work of the type described in this article is making a vital contribution to the understanding of heteroepitaxial-layer evolution during growth and annealing procedures.

References

1. F.C. Frank and J.H. van der Merwe, *Proc. Roy. Soc. A* **200** (1949) p. 125.
2. W.A. Jesser and J.W. Matthews, *Phil. Mag.* **15** (1967) p. 1097.
3. R.J. Asaro and W.A. Tiller, *Metall. Trans.* **3** (1972) p. 1789.
4. M.A. Grinfeld, *Sov. Phys. Dokl.* **31** (1986) p. 831.
5. D.J. Srolovitz, *Acta Metall.* **37** (1989) p. 621.
6. H. Gao, *Int. J. Solids Struct.* **28** (1991) p. 703.
7. P. Nozières, in *Solids Far from Equilibrium*, edited by C. Godrèche (Cambridge University Press, New York, 1992).
8. W.H. Yang and D.J. Srolovitz, *Phys. Rev. Lett.* **71** (1993) p. 1593.
9. J. Grilhé, *Acta Metall. Mater.* **41** (1993) p. 909.
10. M.A. Grinfeld, in *Thermodynamic Methods in the Theory of Heterogeneous Systems* (Longman, New York, 1991).
11. B.J. Spencer, P.W. Voorhees, and S.H. Davies, *Phys. Rev. Lett.* **67** (1991) p. 3696.
12. M.A. Grinfeld, in *Thin Films: Stresses and Mechanical Properties III*, edited by W.D. Nix, J.C. Bravman, E. Arzt, and L.B. Freund (Mater. Res. Soc. Symp. Proc. **239**, Pittsburgh, 1992) p. 183.
13. B.J. Spencer, P.W. Voorhees, and S.H. Davis, *J. Appl. Phys.* **73** (1993) p. 4955.
14. A.J. Pidduck, D.J. Robbins, and A.G. Cullis, in *Microscopy of Semiconducting Materials 1993*, edited by A.G. Cullis, J.L. Hutchison, and A.E. Staton-Bevan (IOP Publishing, Bristol, 1993) p. 609.
15. C-H. Chiu and H. Gao, *Int. J. Solids Struct.* **30** (1993) p. 2983.
16. B.J. Spencer and D.I. Meiron, *Acta Metall. Mater.* **42** (1994) p. 3629.
17. H. Gao, *J. Mech. Phys. Solids* **42** (1994) p. 741.
18. S. Christiansen, M. Albrecht, H.P. Strunk, P.O. Hansson, and E. Bauser, *Appl. Phys. Lett.* **66** (1995) p. 574.
19. A.G. Cullis, D.J. Robbins, A.J. Pidduck, and P.W. Smith, in *Microscopy of Semiconducting Materials 1991*, edited by A.G. Cullis and N.J. Long (IOP Publishing, Bristol, 1991) p. 439.
20. A.G. Cullis, D.J. Robbins, A.J. Pidduck, and P.W. Smith, *J. Cryst. Growth* **123** (1992) p. 333.
21. A.J. Pidduck, D.J. Robbins, A.G. Cullis, W.Y. Leong, and A.M. Pitt, *Thin Solid Films* **222** (1992) p. 78.
22. D. Dutartre, P. Warren, F. Chollet, F. Gisbert, M. Bérenguer, and I. Berbézier, *J. Cryst. Growth* **142** (1994) p. 78.
23. A.G. Cullis, D.J. Robbins, S.J. Barnett, and A.J. Pidduck, *J. Vac. Sci. Technol. A* **12** (1994) p. 1924.
24. Y-W. Mo, D.E. Savage, B.S. Swartzentruber, and M.G. Lagally, *ibid.* **65** (1990) p. 1020.
25. D.E. Jesson, S.J. Pennycook. J-M. Baribeau, and D.C. Houghton, *ibid.* **71** (1993) p. 1744.
26. P.R. Berger, K. Chang, P. Bhattacharya, J. Singh, and K.K. Bajaj, *Appl. Phys. Lett.* **53** (1988) p. 684.
27. G.J. Whaley and P.I. Cohen, *ibid.* **57** (1990) p. 144.
28. S. Guha, A. Madhukar, and K.C. Rajkumar, *ibid.* p. 2110.
29. C.W. Snyder, B.G. Orr, D. Kessler, and L.M. Sander, *Phys. Rev. Lett.* **66** (1991) p. 3032.
30. A.G. Cullis, A.J. Pidduck, and M.T. Emeny, in *Microscopy of Semiconducting Materials 1995*, edited by A.G. Cullis and A.E. Staton-Bevan (IOP Publishing, Bristol, 1995) p. 163.
31. A.G. Cullis, A.J. Pidduck, and M.T. Emeny, *J. Cryst. Growth* **158** (1996) p. 15.
32. D.J. Eaglesham and M. Cerullo, *Phys. Rev. Lett.* **64** (1990) p. 690.
33. T. Walther, C.J. Humphreys, A.G. Cullis, and D.J. Robbins, *Mater. Sci. Forum* **196–201** (1995) p. 505.
34. Q. Xie, A. Madhukar, P. Chen, and N.P. Kobayashi, *Phys. Rev. Lett.* **75** (1995) p. 2542.
35. A. Ponchet, A. Rocher, A. Ougazzaden, and A. Mircea, *J. Appl. Phys.* **75** (1994) p. 7881.
36. J.E. Guyer and P.W. Voorhees, *Phys. Rev. Lett.* **74** (1995) p. 4031.
37. Y.H. Xie, G.H. Gilmer, C. Roland, P.J. Silverman, S.K. Buratto, J.Y. Cheng, E.A. Fitzgerald, A.R Kortan, S. Schuppler, M.A. Marcus, and P.H. Citrin, *Phys. Rev. Lett.* **73** (1994) p. 3006.
38. A.G. Cullis, A.J. Pidduck, T. Martin, and A.D. Johnson, *Appl. Phys. Lett.* (in press).
39. L.B. Freund, A. Bower, and J.C. Ramirez, in *Thin Films: Stresses and Mechanical Properties*, edited by J.C. Bravman, W.D. Nix, D.M. Barnett, and D.A. Smith (Mater. Res. Soc. Symp. Proc. **130**, Pittsburgh, 1989) p. 139.
40. J. Tersoff and F.K. LeGoues, *Phys. Rev. Lett.* **72** (1994) p. 3570.
41. A.G. Cullis, A.J. Pidduck, and M.T. Emeny, *ibid.* **75** (1995) p. 2368.
42. Y. Androussi, A. Lefebvre, C. Delamarre, L.P. Wang, A. Dubon, B. Courboulès, C. Deparis, and J. Massies, *Appl. Phys. Lett.* **66** (1995) p. 3450.
43. J.R. Rice and G.E. Beltz, *J. Mech. Phys. Solids* **42** (1994) p. 333.
44. M. Albrecht, S. Christiansen, J. Michler, W. Dorsch, H.P. Strunk, P.O. Hansson, and E. Bauser, *Appl. Phys. Lett.* **67** (1995) p. 1232.
45. D.E. Jesson, K.M. Chen, S.J. Pennycook, T. Thundat, and R.J. Warmack, *Science* **268** (1995) p. 1161.